Published in final edited form as:
Brain Res. 2008 March 4; 1197: 13–22. doi:10.1016/j.brainres.2007.12.058.

Localization in Stereocilia, Plasma Membrane, and Mitochondria Suggest Diverse Roles for NMHC-IIa Within Cochlear Hair Cells

Anil K. Lalwani[1,4], **Graham Atkin**[1,2], **Yan Li**[1,2], **Jennifer Y. Lee**[1,2], **Dean E. Hillman**[3,4], and **Anand N. Mhatre**[2,4]

[1]Laboratory of Molecular Otology, Department of Otolaryngology, New York University School of Medicine, New York, NY 10016, USA

[2]Laboratory of Molecular Genetics, Department of Otolaryngology, New York University School of Medicine, New York, NY 10016, USA

[3]Department of Otolaryngology, New York University School of Medicine, New York, NY 10016, USA

[4]Department of Physiology and Neuroscience, New York University School of Medicine, New York, NY 10016, USA

Abstract

NMHC-IIA, a nonmuscle myosin heavy chain isoform encoded by *MYH9*, is expressed in sensory hair cells and its dysfunction is associated with syndromic and nonsyndromic hearing loss. In this study, we investigate the ultrastructural distribution of NMHC-IIa within murine hair cells to elucidate its potential role in hair cell function. Using previously characterized anti-mouse NMHC-IIa antibody detected with immunogold labelling, NMHC-IIa was observed in the stereocilia, in the cytosol along the plasma membrane, and within mitochondria. Within stereocilia, presence of NMHC-IIa is observed throughout its length along the actin core, from the center to the periphery and at its base in the cuticular plate, suggesting a potential role in structural support. Within the sensory hair cells, NMHC-IIa was distributed throughout the cytoplasm and along the plasma membrane. A novel finding of this study is the localization of NMHC-IIa within the mitochondria, with the majority of the label along its inner membrane folds. The presence of NMHC-IIa within heterogeneous areas of the hair cell suggests that it may play different functional roles in these distinct regions. Thus, mutant NMHC-IIa may cause hearing loss by affecting hair cell dysfunction through structural and or functional disruption of its stereocilia, plasma membrane, and/or mitochondria.

INTRODUCTION

Mutations of *MYH9* (MIM *160775), encoding a 220 kDa nonmuscle myosin heavy chain-A (NMHC-IIA) are linked to syndromic or nonsyndromic hereditary hearing loss (HHL). The syndromic hearing loss is classified under a family of related disorders known as hereditary

Correspondence to: Anil K. Lalwani, MD, Mendik Foundation Professor and Chairman, Department of Otolaryngology, New York University School of Medicine, 550 First Avenue, NBV-5E5, New York, NY 10016, Tel: 212 263 6344, Fax: 212 263 8257, E-mail: anil.lalwani@nyumc.org. Anand N. Mhatre, PhD, Assistant Professor, Department of Otolaryngology, New York University School of Medicine, 560 First Ave., TCH 513, New York, NY 10016, Tel: 212-263-7686, Fax: 212-263-8150, E-mail: a.mhatre@med.nyu.edu.

macrothrombocytopenias (MTCPs), predominantly characterized by platelet abnormalities [1]; associated clinical symptoms may include nephritis and/or cataracts [16]. To date, the nonsyndromic hearing loss (MIM #603622) has been linked to a single *MYH9* mutant allele, $MYH9^{R705}$ (MIM +160775.0008), which has been identified in two unrelated families with autosomal dominant HHL [9,12]. Hearing dysfunction in the affected individuals is characterized by its delayed onset of progressive high frequency hearing loss with normal platelets [13].

The hearing loss associated with *MYH9* mutations suggests a critical functional role for NMHC-IIA in the auditory organ. Within the cochlea, NMHC-IIa has been localized within the spiral ligament, a connective tissue that serves to anchor the stria vascularis to the lateral wall of the cochlear duct [13]. The spiral ligament is physically and functionally linked to the basilar membrane upon which rests the organ of Corti, the auditory sensory organ containing hair cells. NMHC-IIa has also been immuno-localized within the hair cells and their stereocilia through the use of fluorescent confocal microscopy, identifying them as potential cellular targets of NMHC-IIa dysfunction [18]. The exact role of *MYH9* in hearing and the mechanism of hearing loss due to MYH9 mutation remains to be deciphered.

The embryonic lethality of mice homozygous for the *Myh9* null allele, while emphasizing its critical role in development [3,15,19,22] has precluded analysis of NMHC-IIa dysfunction on cochlear function and structure, particularly at the level of the sensory hair cells. In absence of a knock-out mouse model, transgenic mice expressing dominantly inherited mutant alleles linked to HHL are being generated to understand the role of NMHC-IIa in hearing, platelet development and renal function. Nonetheless, the eventual interpretation of *in vivo* findings within the auditory system will require the precise knowledge of sub-cellular localization of *MYH9* within cochlear tissues. Given the primary role of hair cells in mechanotransduction and hearing, determining MYH9 localization within the hair cells is critical in dissecting its role in hearing. The purpose of this study was to determine the subcellular distribution of MYH9 in hair cells using electron microscopy that will further our understanding of its potential role in hair cell function. Subcellular localization will also enable comparison to the ultrastructural distribution pattern of other myosins linked to HHL and their putative biological roles.

RESULTS

The distribution of NMHC-IIa within murine hair cells in the organ of Corti was assessed through the use of two separate antibodies, an anti-mouse NMHC-IIa polyclonal antibody [18] as well as an anti-NMHC-IIA polyclonal antibody [12,17], and visualized through Transmission Electron Microscopy (TEM). Similar patterns of immunoreactivity were detected with both antibodies within the sterocilia, cytoplasm, plasma membrane, and mitochondria.

I. Distribution of NMHC-IIa in the Stereocilia

Longitudinal sections of hair bundles from murine hair cells (Figure 1 **and** Figure 2) reveal NMHC-IIa immunoreactivity distributed throughout the length of the stereocilia in all three rows. Label is found both at the central core region as well as the periphery of the shaft (Figure 2, A–D). Sections cut through the horizontal plane of the hair bundle (Figure 2, E–G) corroborate these results. Continuous with its distribution along the stereocilia, within the core as well as its periphery, NMHC-IIa immunoreactivity was also associated with its rootlets, extending through the cuticular plate at the apical region of the hair cell and the surrounding matrix (Figure 1B). NMHC-IIa immunoreactivity was not observed at the tips of the stereocilia.

II. Distribution of NMHC-IIa in the Sensory Hair Cells

NMHC-IIa immunoreactivity is distributed throughout the cytoplasm and along the plasma membrane (Figure 3 **and** Figure 4). The distribution pattern of NMHC-IIa associated with the plasma membrane was not homogeneous, i.e., the frequency and location of the immunogold label varied at different points along the lipid bilayer.

Presence of NMHC-IIa was also detected throughout the mitochondria of the sensory hair cells (Figure 4). The mitochondria in the TEM are distinguished both by their classic alignment along the lateral periphery and subnuclear regions of the hair cell as well as by their striated pattern, corresponding to the light and dark alternating rows of cristae and the matrix separated by invaginations of the mitochondrial inner membrane. Distribution of NMHC-IIa immunoreactivity within mitochondria (n=30) was characterized as previously described [27]: 50% of immunoreactivity was observed in the Cristae Membrane (CM) zone, 34% in the Outer Membrane/Inner Boundary Membrane (OM/IBM) zone, and 16% in the matrix. Thus, over four-fifths of NMHC-IIa was associated with the mitochondrial inner membrane.

These results from EM localization studies within the stereocilia, mitochondria, and sensory hair cells are schematized in Figure 5 **and** Figure 6 respectively.

III. Identification of NMHC-IIa in the cochlear mitochondrial fractions

Presence of NMHC-IIa within mitochondria was also corroborated through Western blot analysis of the cochlear and kidney mitochondrial fractions (Figure 7). The anti-NMHC-IIa antibody identified a single immunoreactive band of 220 kDa in the protein homogenate from the whole cell extract. The whole cell extract is positive for glyceraldehyde 3-phosphate dehydrogenase (GAPDH), a cytoplasmic marker protein, and cytochrome C, a mitochondrial marker protein. The mitochondrial fraction, separated from the cochlear or kidney whole cell extract, is also positive for the 220 kDa NMHC-IIA and Cytochrome C but not GAPDH, confirming the relative purity of the mitochondrial fraction and absence of contaminating cytosolic proteins.

DISCUSSION

This study describes ultrastructural immuno-localization of NMHC-IIa in murine sensory hair cells, using previously characterized polyclonal antibodies against the mouse NMHC-IIa [18] and human NMHC-IIA [13,17] yielding complete overlap in their immunoreactivities. NMHC-IIa was localized within the stereocilia, the cuticular plate and its surrounding matrix, the cytoplasm, plasma membrane, and mitochondria. Presence of NMHC-IIa within the mitochondria, corroborated through Western blot analysis of mitochondrial fractions, and particularly its association with the inner membrane, demonstrated through immunogold localization studies, has not been previously documented.

The transduction of sound by the hair cells is critically dependent upon structural and functional integrity of its stereocilia. The stereocilia are specialized protrusions of the plasma membrane containing bundles of actin filaments anchored basally to luminal surface of the sensory cells [14,28]. Movement of the stereocilia relative to each other triggers the transduction of the sound stimulus into electrical signals directed to the brain. Important constituents of the stereocilia include several members of the large myosin family that have been shown to play a critical role in their differentiation and maintenance of functional integrity. Amongst the seven myosins that have been linked to HHL in humans (Table I), mutant alleles of three myosin orthologues, Myosin VI, Myosin VIIa and Myosin XVa have been identified in mouse models of hearing loss: all three of these myosins have been localized to the sensory hair cells. Mouse strains homozygous for mutant alleles encoding any one of these three myosins show a general

deformation of their hair bundles [8,10] thus supporting their role in the differentiation and morphogenesis of the individual hair cells.

The ultrastructural distribution pattern of NMHC-IIA within the stereocilia is distinct from the other four myosins linked to HHL and characterized for their distribution in the hair cells through TEM (**See** Table 1 **and** Figure 5). NMHC-IIA is distributed throughout the length of the stereocilia occupying both the central core region as well as the periphery of the shaft suggesting distinct functions at these two locations. In addition, NMHC-IIa is also present within the rootlets of the stereocilia that extend into the cuticular plate where it may play a potential role in structural support of these projections. While NMHC-IIa is extensively distributed throughout the length, it is conspicuously absent from the tips of the stereocilia, where other myosins, including myosin XVa, have been localized. Exclusion from the tips of the stereocilia may rule out a role a direct for NMHC-IIa in the function of the transduction channel.

Plasma membrane localization of NMHC-IIa within the hair cell, as demonstrated by the current study, is consistent with the characterization of its distribution in other cell types and non-TEM-based studies. Direct support for membrane localization has been provided by co-purification and binding studies as well as physiological investigations. Nearly half of nonmuscle myosin II harvested from axoplasm of the squid giant axon co-purified with axoplasmic organelles suggesting its membrane association and a role in transport of organelles [5]. The specific biological role played by the membrane-associated NMHC-IIA is currently under intense study. It is speculated that membrane localization renders the NMHC-IIa with attributes of a signal transducer that can link external stimuli to alterations in the cytoskeleton, thus effecting changes in cell structure and function. These include receptors for angiotensin converting enzyme (ACE) [11], considered to play a critical role in the regulation of blood pressure and Lipoxins (LXs) [24], endogenous anti-inflammatory mediators that promote phagocytosis of apoptotic PMN by macrophages *in vitro* and *in vivo*.

In vitro studies using liposomes have shown that nonmuscle myosin II isoforms bind to the plasma membrane via the COOH-terminal regions of its heavy chain with variable affinity [20]. Phosphorylation of the nonmuscle myosin II tail domain is considered to modulate its membrane association; binding of the nonmuscle myosin heavy chain II tail domain to the phosphotidylserine liposomes was associated with phosphorylation of its tail domain by protein kinase C [21]. Similarly, Ben-Ya'acov et al (2003) demonstrated that EGF-induced chemotaxis is mediated through phosphorylation of NMHC-IIa and its isoform NMHC-IIb, which regulates their subcellular localization [2].

Similar to its localization within the cytoplasm and along the plasma membrane, NMHC-IIa is also found within the matrix and membranes of the mitochondria, as demonstrated by electron microscopy and corroborated by Western blot analysis of fractionated cochlear and renal mitochondria (**See** Figure 6). Presence of NMHC-IIa within the mitochondria raises the novel possibility that clinical symptoms linked to *MYH9* mutations may be a consequence of mitochondrial dysfunction. Interestingly, the presence within the mitochondria has not been reported for any of the other myosins linked to HHL.

A significant fraction of the mitochondrial NMHC-IIa is localized to the inner membrane. The mitochondrial inner membrane is distinguished from the plasma membrane by its relatively greater protein-to-lipid mass ratio and a unique set of multi-unit protein complexes that carry out fundamental processes related to energy production (e.g., Krebs cycle or oxidative phosphorylation). Co-immunoprecipitation studies from our own laboratory seeking to isolate NMHC-IIa associated proteins have identified two mitochondrial proteins encoded by nuclear genome: oxoglutarate dehydrogenase (OGDH) and a mitochondrial ATP-dependent protease,

Lon (Unpublished Results). OGDH is part of the multi-enzyme alpha-ketoglutarate dehydrogenase complex that catalyzes a key reaction in the Krebs tricarboxylic acid cycle. Due to different functions of the plasma and mitochondrial membranes and their distinct protein compositions, it is likely that membrane associated NMHC-IIa's role in the mitochondria is distinct from its role in the cytoplasm.

In summary, NMHC-IIa is distributed within distinct regions of the cochlear sensory hair cell. These include the stereocilia, cuticular plate, cytoplasm, plasma membrane and the mitochondrial matrix and inner membrane. Presence within the plasma membrane and the cristae support noncontractile function for the membrane-associated form of the NMHC-IIa. Presence within the stereocilia raises the possibility that hearing loss linked to NMHC-IIa mutations may be a consequence of abnormality or pathology of the sterocilia that leads to failure in mechanotransduction.

EXPERIMENTAL PROCEDURES

Animals and Antibodies

CD1 and FVB/n mice, 6 to 8 weeks old, were used as the animal models in the current study. All procedures involving the animals were approved by the IACUC at NYU SoM. Two different polyclonal antibodies were used to study the subcellular distribution of NMHC-IIa within the hair cell to allow comparison and confirmation of results. The first antibody, a rabbit anti-mouse NMHC-IIa polyclonal antibody, was prepared by Proteintech Group Inc. (www.ptglab.com) against a 18-amino acid-long peptide fragment, SDEEVDGKADGADAKAAE, corresponding to the mouse *Myh9* C-terminal sequence [gi: 20137005] [4,17]. The derivation of the immunogenic peptide was based on the peptide fragment used in generation of isoform-specific antibody against *MYH9* [23]. The anti-mouse NMHC-IIa polyclonal antibody has been characterized, for its activity and specificity, and applied towards NMHC-IIa immunolocalization studies [18]. The second antibody used was a commercially available polyclonal antibody against purified myosin from human platelets (Biomedical Technologies, BTI-561). This antibody has been previously used to assess localization of NMHC-IIa within cochlear sections from the rat as well as the mouse [12,17].

Fixation, Embedding and Sectioning

Adult CD1 mice were anesthetized with ketamine (0.1 mg/g i.p.) and xylazine (0.001 mg/g i.p.) and perfused systemically through the aorta, initially with a flush of phosphate-buffered saline (PBS) (pH 7.5, 0.15 M) followed by paraformaldehyde fixative (4% in PBS). Immediately after perfusion, the animals were decapitated and their temporal bones removed. These temporal bones were dissected to expose the cochleae, which were opened at the apex of the otic capsule and the round window. The cochleae were then post-fixed in 4% PFA for two hours at room temperature, washed 3 times for 10 minutes in PBS, and placed in a 1.25 M EDTA in PBS (pH 7.4) at room temperature for 24 hours. Cochleae were then rinsed 3 times for 10 minutes in PBS, and then in distilled water for 3 times for 5 minutes. Cochleae were dehydrated in a series of graded alcohols: 70%, 80%, 90% ETOH for ten minutes each, and 100% ETOH for 30 minutes. Tissues were then placed into LR White Resin (medium grade, London Resin Company, Ltd.) for one hour at room temperature. The resin was exchanged for fresh resin and the tissues were infiltrated overnight at four degrees. A final change to fresh resin was made the next morning, and the tissues were embedded in filled, tightly-capped gelatin capsules (size 00, Parr Instrument Company). These capsules were incubated at 51.5 degrees for 24 hours.

Blocks were cut on a Leica UCT microtome with a Diatome diamond knife. Ultrathin sections, 70nm thick, taken in either horizontal or radial planes, were collected on single-slot formvar

copper grids (Electron Microscopy Sciences). The following day, sections were rehydrated in PBS (pH 7.4) for 10 minutes (each grid was placed section-side down on a single drop of liquid), and then placed in a blocking solution of fresh 1% BSA in PBS for 1 hour at room temperature.

Immunocytochemical Labeling and Detection

Grids were labeled in a moist chamber by incubation with either rabbit polyclonal anti-non-muscle myosin II-A antibody, diluted 1:2000 in BSA blocking solution, or anti-human-NMHC-IIa antibody (Biomedical Technologies, BTI-561), diluted 1:1000 in BSA blocking solution, at 4 °C for 16 hours. Grids were then washed 6x for 5 minutes each in PBS, and then the bound label detected by incubating with goat anti-rabbit Alexa Fluor 488 secondary antibody conjugated to both a fluorophore and colloidal gold (colloidal gold size 10 nm from Molecular Probes) or 18nm Colloidal Gold-AffiniPure Goat Anti-Rabbit IgG (H+L) (from Jackson Immunoresearch, 111-215-144), diluted 1:20 in PBS, for 1 hour at room temperature. Grids were again washed 6 × 5 minutes in PBS, followed by 3 × 5 minutes in distilled water. To enhance contrast and visualization of the sections, grids were then briefly stained for 5–10 minutes in uranyl acetate, washed in distilled water, stained for 5–10 minutes in lead citrate, washed again in distilled water, and dried. Controls were performed to check the immunolabelling procedures, wherein grids were processed as above without primary antibody and examined under EM. These control grids were relatively free of the gold label. Grids were examined with a Phillips CM12 Transmission Electron Microscope and photographed with a 1k × 1k Gatan CCD Camera. The images presented in the study are representative of several different cochleae harvested and characterized from different animals.

Assessment of the Immunogold Label in Mitochondria

Gold label distribution in mitochondria was assessed and quantified as described by Vogel et al. [27]. Briefly, three sub-regions of the mitochondria were defined: the cristae membrane zone (CM), the outer membrane/inner boundary membrane zone (OM/IMB), and the matrix. Label was deemed to be within the cristae membrane zone if the center of that gold particle was ≤ 14nm from the cristae membrane and not in the OM/IMB zone; within the OM/IMB zone if ≤ 14nm from the OM or IMB; within the matrix if > 14nm from the CM and OM/IMB zones. Label was counted from thirty mitochondria using Adobe Photoshop CS2 and Microsoft Excel 2001.

Mitochondrial Fractionation and Western Blot Analysis

Presence of NMHC-IIa within the mitochondria was also assessed by mitochondrial fractionation from cochlea and kidney followed by Western blot analysis of protein extracts. All reagents were obtained from Pierce Biotechnology (Rockford, IL) unless otherwise noted.

Kidney and cochleae tissue samples were harvested from adult FVB/n mice and frozen immediately on dry ice. The tympanic bulla was removed from each cochlea to expose the otic capsule; twenty cochleae dissected in this way were homogenized in PBS containing complete protease inhibitor (one tablet per 50 mL, Roche, Indianapolis, IN) and using a metal pulverizer, pre-chilled with liquid nitrogen. The kidney homogenate was similarly prepared.

The homogenates were fractionated by serial centrifugation at 3000 × g for 10 minutes to remove nuclei, followed by 6800 × g for 15 minutes to pellet the mitochondria. Mitochondria pellets were re-suspended in PBS containing protease inhibitor (one tablet per 50 mL, Roche, Indianapolis, IN). Protein concentration was determined using a Lowry detergent compatible protein assay (Biorad, Hercules, CA). Mitochondrial fractions and whole tissue extracts were boiled in SDS sample buffer for 5 minutes and resolved on a 1.0 mm-thick, 4–12% NuPAGE Bis-Tris minigel via electrophoreses at 200 V for 60 minutes in NuPAGE MOPS running buffer

(Invitrogen, Carlsbad, CA). The gel was transferred to a nitrocellulose membrane at 40 V for 60 minutes in NuPAGE Transfer buffer (Invitrogen, Carlsbad, CA). The membrane was treated with 0.3% I-Block (Tropix, Bedford, MA) in PBS at 4°C overnight to block non-specific binding sites, and then incubated with anti-mouse-NMHC-IIa antibody diluted 1:3,000 in blocking buffer at room temperature for 1.5 hours. The blot was washed in PBS with 0.1% Triton-100 followed by incubation with horse-radish peroxidase (HRP)-conjugated, goat anti-rabbit IgG (Vector Laboratories, Burlingame, CA) at room temperature for 1 hour. The blot was developed using a western blot ECL substrate kit (Pierce) followed by exposure to an autoradiography film Hyperfilm ECL (GE Healthcare, Piscataway, NJ).

ACKNOWLEDGMENTS

This study was supported by the NIDCD (DC005199).

REFERENCES

1. Balduini CL, Iolascon A, Savoia A. Inherited thrombocytopenias: from genes to therapy. Haematologica 2002;87:860–880. [PubMed: 12161364]
2. Ben-Ya'acov A, Ravid S. Epidermal growth factor-mediated transient phosphorylation and membrane localization of myosin II-B are required for efficient chemotaxis. J Biol Chem 2003;278:40032–40040. [PubMed: 12874274]
3. Conti MA, Even-Ram S, Liu C, Yamada KM, Adelstein RS. Defects in cell adhesion and the visceral endoderm following ablation of nonmuscle myosin heavy chain II-A in mice. J Biol Chem 2004;279:41263–41266. [PubMed: 15292239]
4. D'Apolito M, Guarnieri V, Boncristiano M, Zelante L, Savoia A. Cloning of the murine non-muscle myosin heavy chain IIA gene ortholog of human MYH9 responsible for May-Hegglin, Sebastian, Fechtner, and Epstein syndromes. Gene 2002;286:215–222. [PubMed: 11943476]
5. DeGiorgis JA, Reese TS, Bearer EL. Association of a nonmuscle myosin II with axoplasmic organelles. Mol Biol Cell 2002;13:1046–1057. [PubMed: 11907281]
6. Donaudy F, Ferrara A, Esposito L, Hertzano R, Ben-David O, Bell RE, Melchionda S, Zelante L, Avraham KB, Gasparini P. Multiple mutations of MYO1A, a cochlear-expressed gene, in sensorineural hearing loss. Am J Hum Genet 2003;72:1571–1577. [PubMed: 12736868]
7. Garcia JA, Yee AG, Gillespie PG, Corey DP. Localization of myosin-Ibeta near both ends of tip links in frog saccular hair cells. J Neurosci 1998;18:8637–8647. [PubMed: 9786971]
8. Hasson T. Unconventional myosins, the basis for deafness in mouse and man. Am J Hum Genet 1997;61:801–805. [PubMed: 9382088]
9. Hildebrand MS, de Silva MG, Gardner RJ, Rose E, de Graaf CA, Bahlo M, Dahl HH. Cochlear implants for DFNA17 deafness. Laryngoscope 2006;116:2211–2215. [PubMed: 17146397]
10. Karolyi IJ, Probst FJ, Beyer L, Odeh H, Dootz G, Cha KB, Martin DM, Avraham KB, Kohrman D, Dolan DF, Raphael Y, Camper SA. Myo15 function is distinct from Myo6, Myo7a and pirouette genes in development of cochlear stereocilia. Hum Mol Genet 2003;12:2797–2805. [PubMed: 12966030]
11. Kohlstedt K, Kellner R, Busse R, Fleming I. Signaling via the angiotensin-converting enzyme results in the phosphorylation of the nonmuscle myosin heavy chain IIA. Mol Pharmacol 2006;69:19–26. [PubMed: 16186248]
12. Lalwani AK, Goldstein JA, Kelley MJ, Luxford W, Castelein CM, Mhatre AN. Human nonsyndromic hereditary deafness DFNA17 is due to a mutation in nonmuscle myosin MYH9. Am J Hum Genet 2000;67:1121–1128. [PubMed: 11023810]
13. Lalwani AK, Luxford WM, Mhatre AN, Attaie A, Wilcox ER, Castelein CM. A new locus for nonsyndromic hereditary hearing impairment, DFNA17, maps to chromosome 22 and represents a gene for cochleosaccular degeneration. Am J Hum Genet 1999;64:318–323. [PubMed: 9915977]
14. Lin HW, Schneider ME, Kachar B. When size matters: the dynamic regulation of tereocilia lengths. Curr Opin Cell Biol 2005;17:55–61. [PubMed: 15661519]

15. Matsushita T, Hayashi H, Kunishima S, Hayashi M, Ikejiri M, Takeshita K, Yuzawa Y, Adachi T, Hirashima K, Sone M, Yamamoto K, Takagi A, Katsumi A, Kawai K, Nezu T, Takahashi M, Nakashima T, Naoe T, Kojima T, Saito H. Targeted disruption of mouse ortholog of the human MYH9 responsible for macrothrombocytopenia with different organ involvement: hematological, nephrological, and otological studies of heterozygous KO mice. Biochem Biophys Res Commun 2004;325:1163–1171. [PubMed: 15555549]

16. Mhatre AN, Kim Y, Brodie HA, Lalwani AK. Macrothrombocytopenia and progressive deafness is due to a mutation in MYH9. Otol Neurotol 2003;24:205–209. [PubMed: 12621333]

17. Mhatre AN, Li J, Kim Y, Coling DE, Lalwani AK. Cloning and developmental expression of nonmuscle myosin IIA (Myh9) in the mammalian inner ear. J Neurosci Res 2004;76:296–305. [PubMed: 15079858]

18. Mhatre AN, Li Y, Atkin G, Maghnouj A, Lalwani AK. Expression of Myh9 in the mammalian cochlea: localization within the stereocilia. J Neurosci Res 2006;84:809–818. [PubMed: 16862555]

19. Mhatre AN, Li Y, Bhatia N, Wang KH, Atkin G, Lalwani AK. Generation and Characterization of Mice with Myh9 Deficiency. Neuro Molecular Medicine 2007;9:205–215.

20. Murakami N, Elzinga M, Singh SS, Chauhan VP. Direct binding of myosin II to phospholipid vesicles via tail regions and phosphorylation of the heavy chains by protein kinase C. J Biol Chem 1994;269:16082–16090. [PubMed: 8206908]

21. Murakami N, Singh SS, Chauhan VP, Elzinga M. Phospholipid binding, phosphorylation by protein kinase C, and filament assembly of the COOH terminal heavy chain fragments of nonmuscle myosin II isoforms MIIA and MIIB. Biochemistry 1995;34:16046–16055. [PubMed: 8519761]

22. Parker LL, Gao J, Zuo J. Absence of hearing loss in a mouse model for DFNA17 and MYH9-related disease: the use of public gene-targeted ES cell resources. Brain Res 2006;1091:235–242. [PubMed: 16630581]

23. Phillips CL, Yamakawa K, Adelstein RS. Cloning of the cDNA encoding human nonmuscle myosin heavy chain-B and analysis of human tissues with isoform-specific antibodies. J Muscle Res Cell Motil 1995;16:379–389. [PubMed: 7499478]

24. Reville K, Crean JK, Vivers S, Dransfield I, Godson C. Lipoxin A4 redistributes myosin IIA and Cdc42 in macrophages: implications for phagocytosis of apoptotic leukocytes. J Immunol 2006;176:1878–1888. [PubMed: 16424219]

25. Rzadzinska AK, Schneider ME, Davies C, Riordan GP, Kachar B. An actin molecular treadmill and myosins maintain stereocilia functional architecture and self-renewal. J Cell Biol 2004;164:887–897. [PubMed: 15024034]

26. Schneider ME, Dose AC, Salles FT, Chang W, Erickson FL, Burnside B, Kachar B. A new compartment at stereocilia tips defined by spatial and temporal patterns of myosin IIIa expression. J Neurosci 2006;26:10243–10252. [PubMed: 17021180]

27. Vogel F, Bornhovd C, Neupert W, Reichert AS. Dynamic subcompartmentalization of the mitochondrial inner membrane. J Cell Biol 2006;175:237–247. [PubMed: 17043137]

28. Whitlon DS. Cochlear development: hair cells don their wigs and get wired. Curr Opin Otolaryngol Head Neck Surg 2004;12:449–454. [PubMed: 15377960]

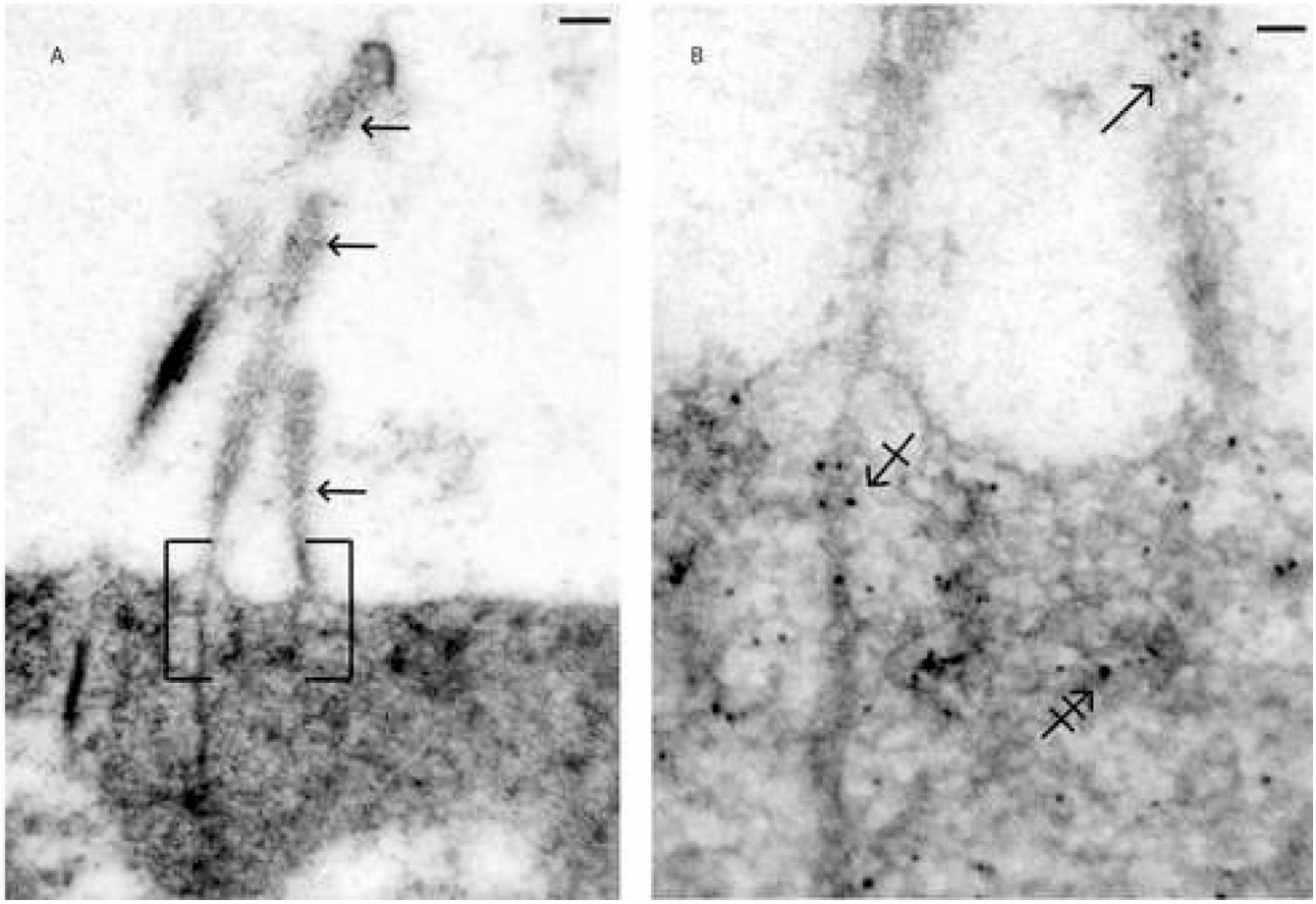

Fig. 1. Distribution of NMHC-IIa in murine cochlear hair bundle and cuticular plate

Ultrastructural distribution of NMHC-IIa within a murine outer hair cell was assessed using a polyclonal anti-NMHC-IIa antibody. Figure 1A depicts a luminal surface of a sensory hair cell projecting its bundle of stereocilia and NMHC-IIa distribution within, e.g., along the length of all 3 rows of stereocilia (arrows). Figure 1B, a magnified subsection of 1A, demonstrates presence of NMHC-IIa within the shaft (arrow), within and around the rootlets (crossed arrow), and throughout the surrounding matrix (double-crossed arrow). Scale bar: 100 nanometers (A), 60 nanometers (B).

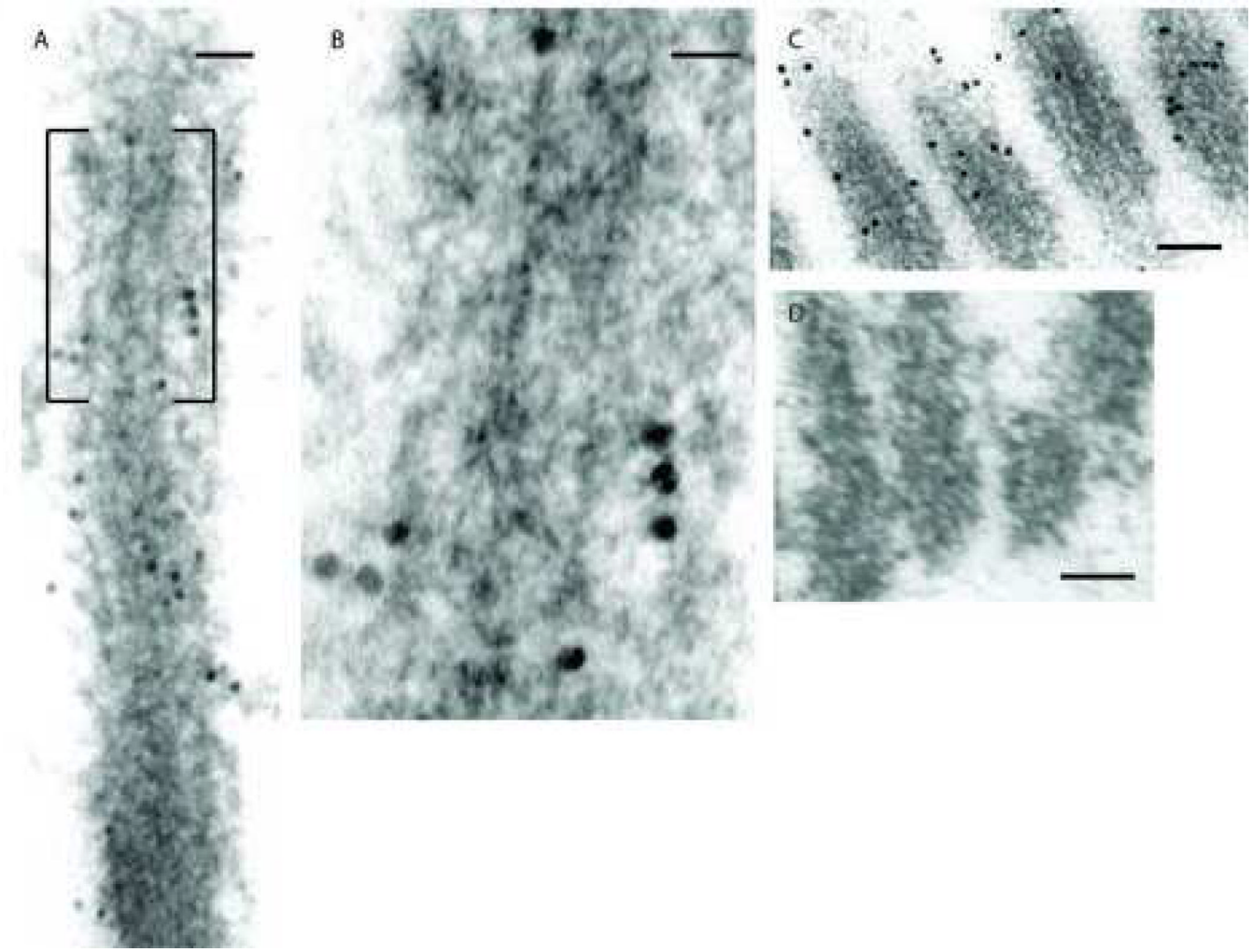

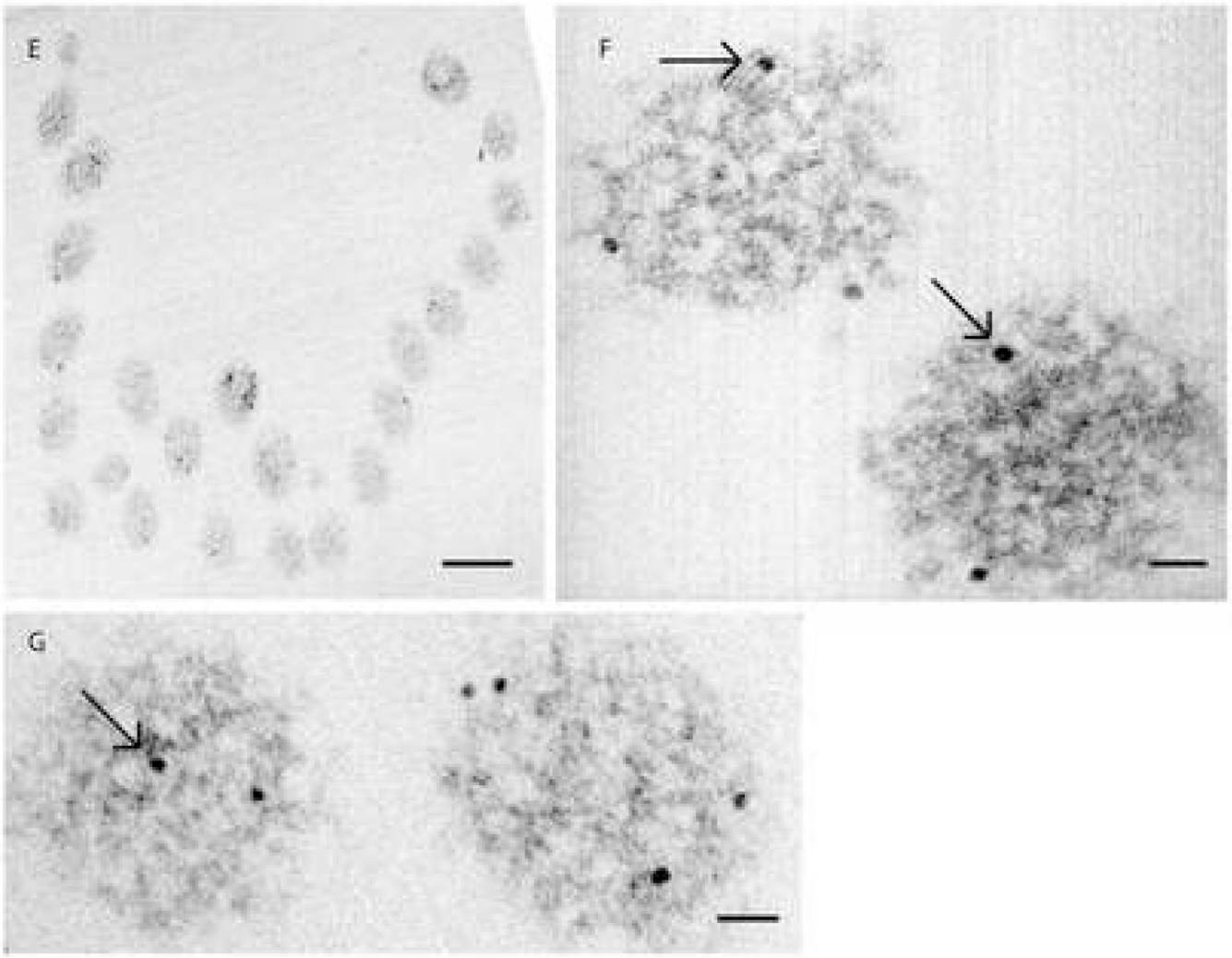

Fig. 2. Distribution of NMHC-IIa within the stereocilia of murine cochlear hair cell

Distribution pattern of NMHC-IIa within the stereocilia was assessed through longitudinal (A, B, C, and D) and horizontal (E, F, and G) sections of the hair bundles with anti-NMHC-IIa antibody. NMHC-IIa distribution is demonstrated throughout the length of the stereocilia, Fig 2A, with a higher prevalence of the protein in the periphery of the shaft than in the central region, Fig 2B. A secondary antibody conjugated with larger gold particles (18nm) was used to detect the bound primary antibody in Fig 2C. In the absence of the primary antibody, the immunogold particles were relatively absent Fig 2D.

Cross-sections cut perpendicular to the long axis of the stereocilia bundle from an outer hair cell illustrate the characteristic “V” pattern, Fig 2E. Within individual stereocilium, NMHC-IIa distribution is observed in two locations: in the periphery of the shaft, Fig 2F(arrow), and, less frequently, at the core of the shaft, Fig 2G (arrow). Scale bars: 50 nanometers (A), 20 nanometers (B), 100 nanometers (C and D), 200 nanometers (E), 30 nanometers (F and G)

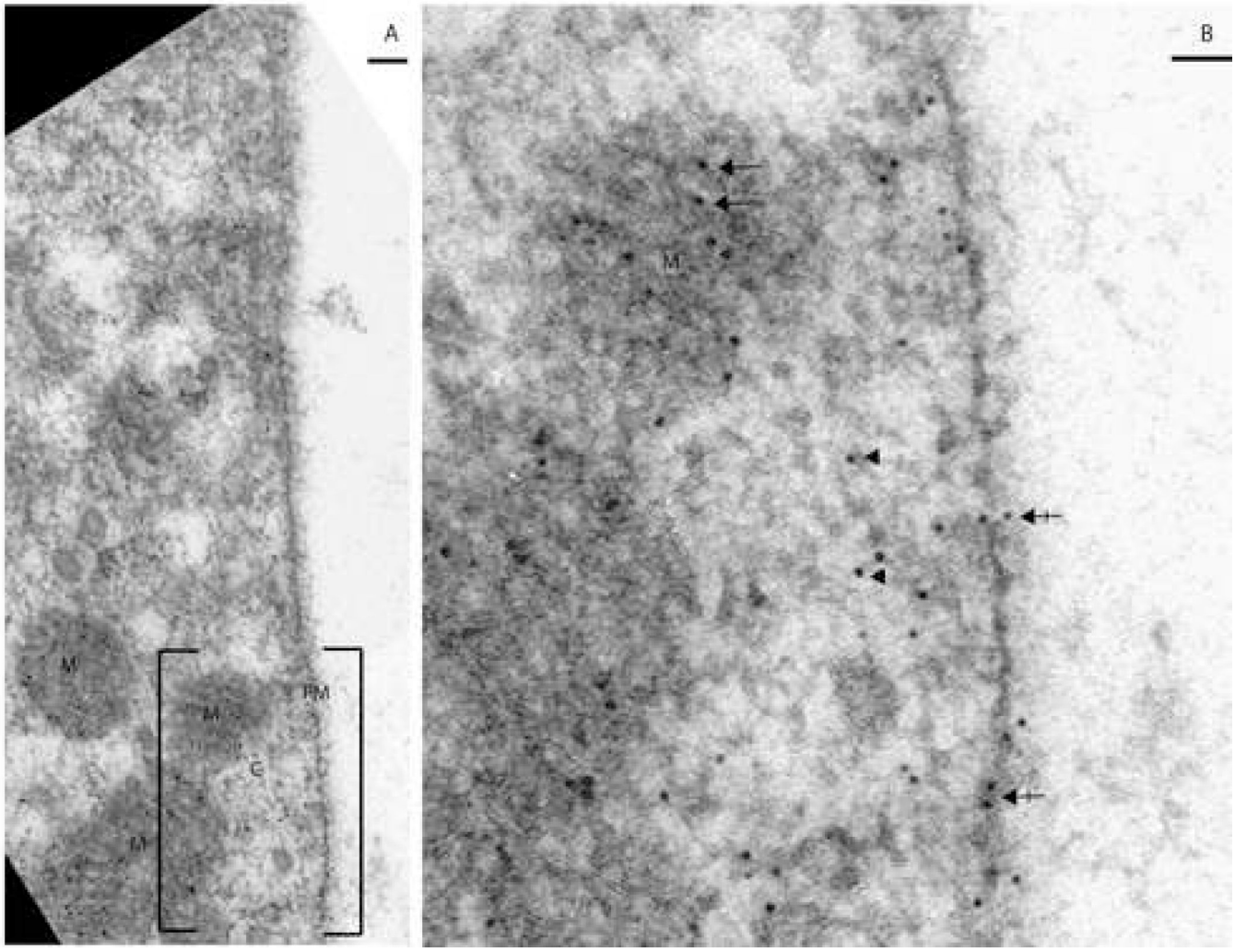

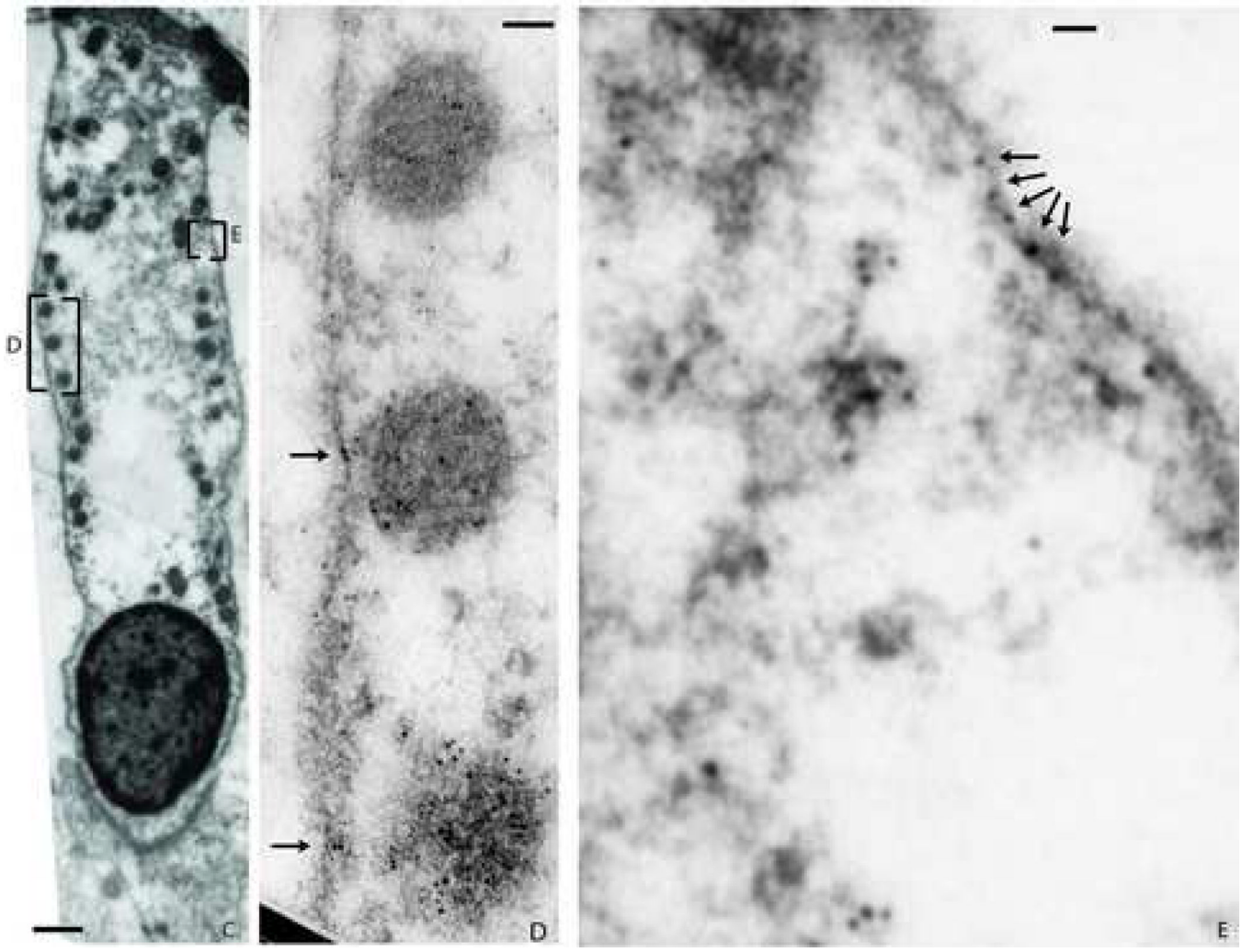

Figure 3. Distribution of NMHC-IIa within murine sensory hair cell

Ultra-thin sections of the mouse cochleae were probed with anti-NMHC-IIa antibody. The target- bound antibody was detected with a secondary antibody conjugated to 10 nanometer gold particles. The bound label was visualized through transmission electron microscopy (TEM) of ultra-thin sections of mouse cochleae.

Transmission electron photomicrograph in Fig 3A demonstrates NMHC-IIa immunoreactivity within the sensory hair cell localized to the cytoplasm (C), mitochondria (M), and the plasma membrane (PM). A magnified inset from 3A demonstrates localization of the nanogold particle label in the cytoplasm (arrowheads), mitochondria (arrows), and to the plasma membrane (crossed arrows). Figure 3C. A murine outer hair cell characterized for immunoreactivity towards anti-NMHC-IIa antibody and its magnified insets (D and E) illustrating the abundance of label co-localized to plasma membrane (arrows). Scale bar: 100 nanometers (A), 50 nanometers (B), 1 micron (C), 50 nanometers (D), 30 nanometers (E).

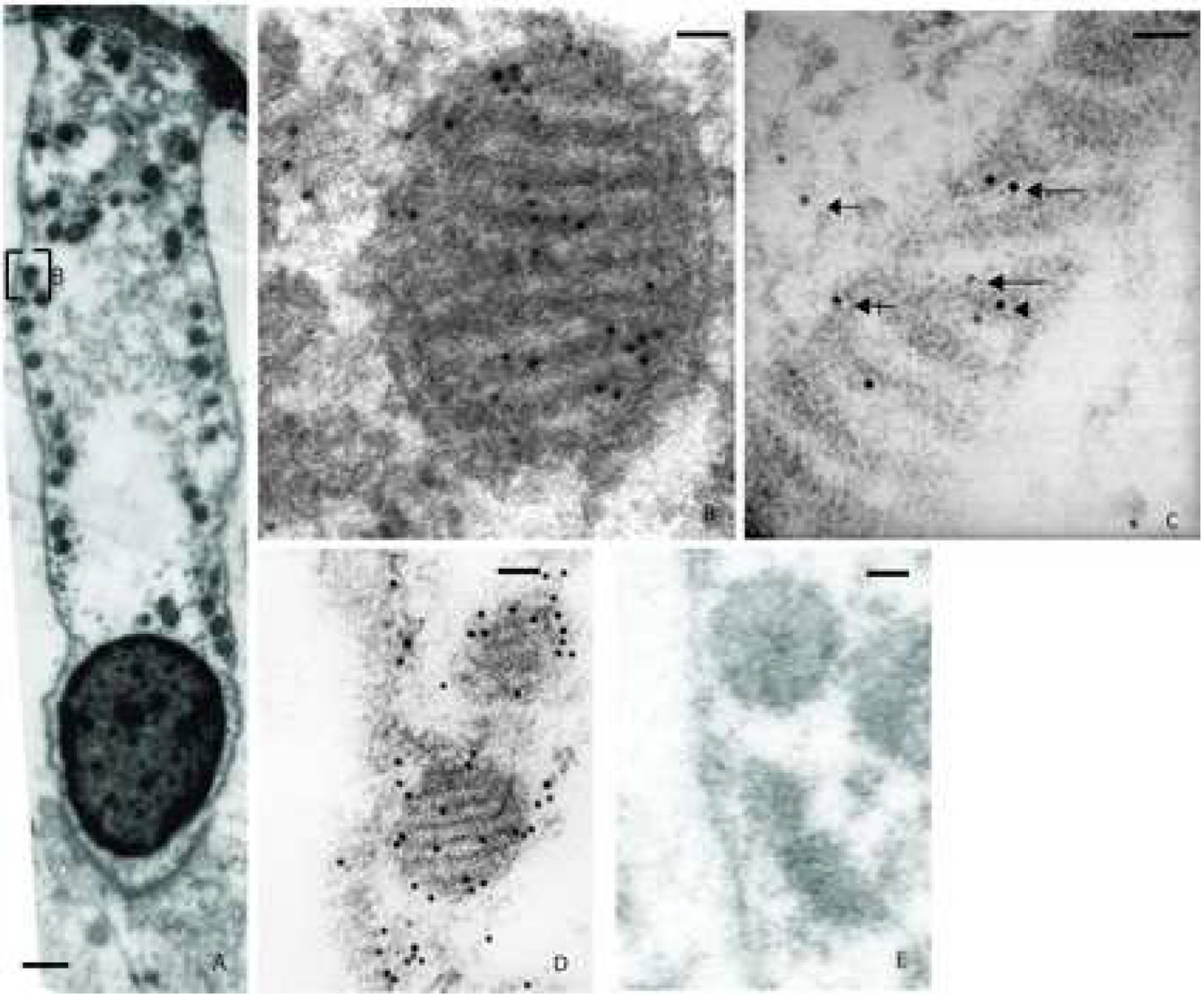

Figure 4. Distribution of NMHC-IIa within the mitochondria from murine sensory hair cell

A. Murine outer hair cell illustrating immunoeactivity towards anti-NMHC-IIa antibody with its mitochondria aligned along the periphery of the cell. B. A magnified subsection of 4A depicts the presence of the immunogold label within the mitochondria. C. A higher magnification image of a mitochondrion illustrating distribution of the nanogold label co-localized to the three established sub-regions within: the cristae membrane zone (long arrows), the matrix (arrowhead), and the outer membrane/ inner boundary membrane zone (crossed arrow). Presence of the nanogold label in the cytoplasm is also denoted (arrow). D. A labeled mitochondrion from sensory hair cell using a secondary antibody conjugated with larger gold particles (18 nm). E. In the absence of the primary antibody, the immunogold particles were relatively absent. Scale bar: 1 micron (A), 50 nanometers (B, and C), 100 nanometers (D and E).

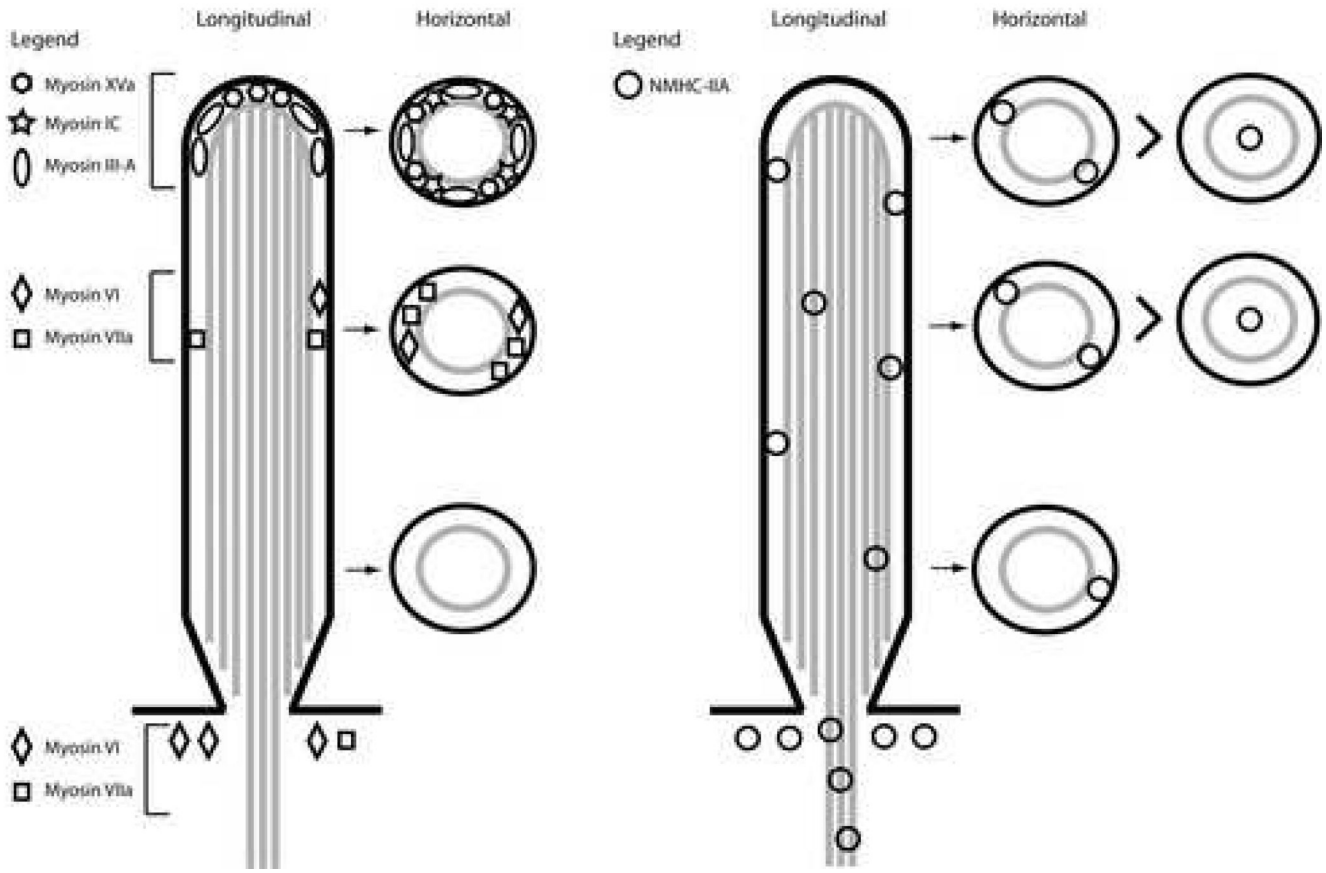

Figure 5. Distribution of myosins within the stereocilia of mammalian cochlear hair cells

Five separate myosins have been localized within the stereocilia of mouse cochlear hair cells. Their longitudinal and horizontal distribution pattern is schematically illustrated in the left half of the panel. The distribution pattern of NMHC-IIA within the stereocilia, as documented in the current studies through TEM and illustrated in the right half of the panel, is distinct from the other myosins and relatively more prevalent.

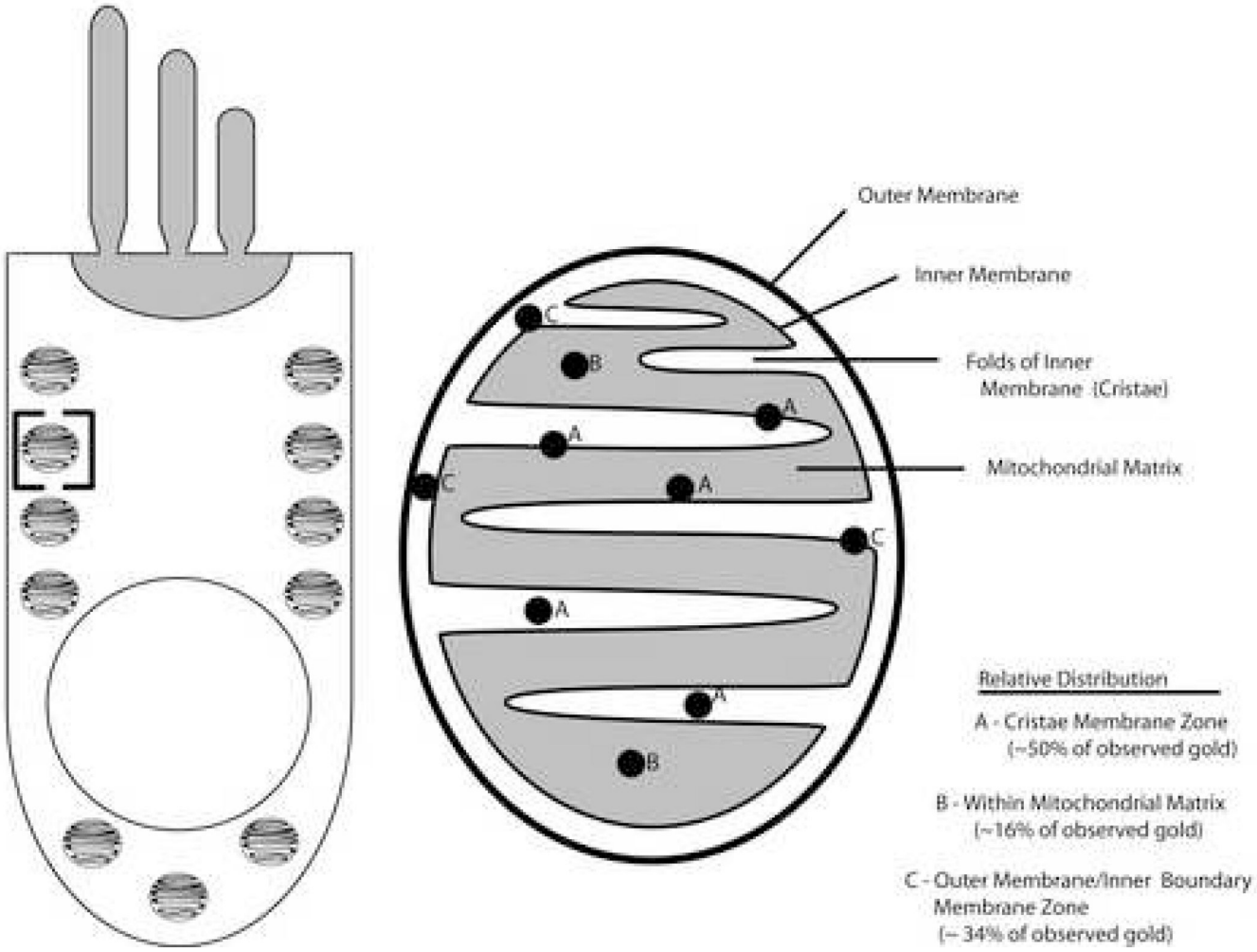

Figure 6. Distribution of NMHC-IIA within the mitochondria of mammalian cochlear hair cells

A schematic depiction of NMHC-IIa distribution within the mitochondria of cochlear hair cells. The schematic in the left half of the panel depicts the body of a sensory hair cell with the characteristic alignment of mitochondria along its lateral membrane. The bracketed region within the schematic is magnified in the right half of the panel and depicts the distribution of NMHC-IIa within the different morphological regions (sub-domains) of the mitochondria. Note that NMHC-IIa is localized predominantly along the inner membrane.

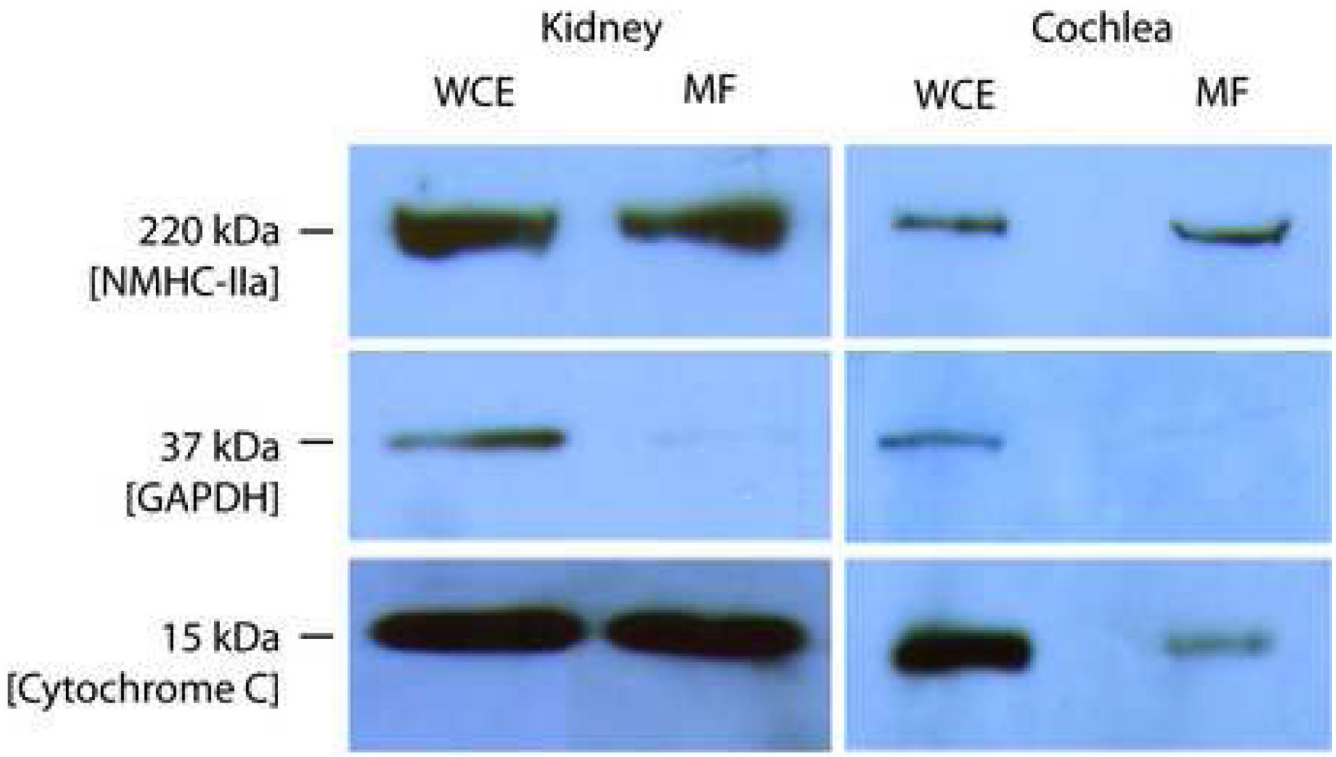

Figure 7. Presence of NMMHC II-a within the protein homogenate from mitochondrial fractions

Immunoblot analysis of protein homogenate from the whole cell extract (WCE) and mitochondrial fractions (MF) isolated from the cochlea and kidney demonstrates presence of 220 kDa NMHC-IIa. The mitochondrial fractions from the cochlea and kidney are positive for presence of the mitochondrial marker Cytochrome C (15 kDa) and negative for cytoplasmic marker GAPDH (37 kDa). The protein homogenate from the whole cell extracts (WCE) from which the mitochondria were fractionated is immuno-positive for NMHC-IIa, GAPDH and Cytochrome C.

Table 1

Myosins Expressed within the Cochlear Sensory Hair cells

Myosin	**Linked to Human Disease**	**Mouse Model**	**Location**	**EM**
Myosin IA (MYO1A)	DFNA48; bilateral HHL, variable [6]	NA	Cochlea	No
Myosin IC (MYO1C)	No	Expressed modified Myosin-1c susceptible to inhibition, supported its essential role in adaptation	At the tips of stereocilia	Yes [7]
Myosin IIIA (MYO3A)	DFNB30; bilateral progressive HHL affecting high frequencies initially	NA	Inner and outer hair cells	Yes [24]
Myosin VI (MYO6)	DFNA22; progressive, post-lingual HHL DFNB37; bilateral, severe to profound, congenital HHL	*Snell's waltzer*, disorganization and fusing of stereociliary bundles	Cuticular plate	Yes [23]
Myosin VIIA (MYO7A)	DFNA11 progressive at all frequencies DFNB2 Usher 1C	*shaker-1*, disorganized bundles	Diffusely throughout the length of the stereocilia, strongly in a band partway up the shaft	Yes [23]
Myosin XVA (MYO15A)	DFNB3, congenital	*Shaker-2* short stereocilia nearly equal in length	At the tips of stereocilia	Yes [23]
MYH9 (NMHC IIA)	DFNA17, Progressive HF HHL, CSD	NA	Hair cells, throughout the length of the stereocilia and the rootlets of the shaft	Yes
MYH14 (NMHC IIC)	DFNA4; progressive	NA	Inner and outer hair cells	No

NA – not available